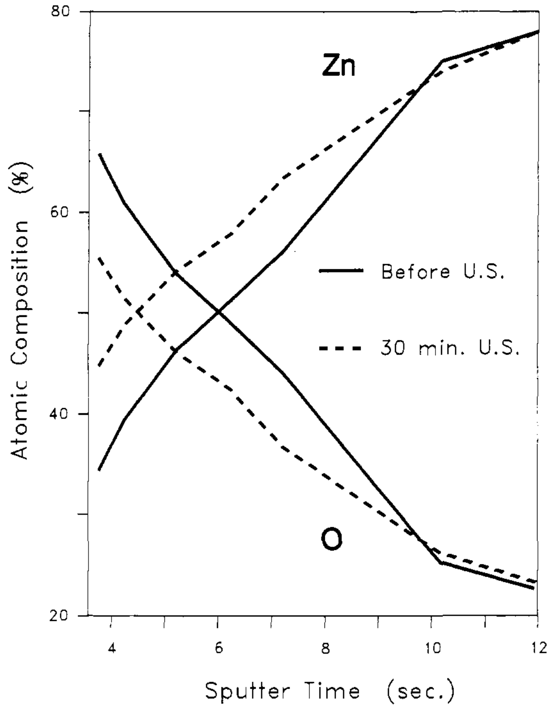

Figure 3. Atomic composition depth profiles of Zn pellets before and after ultrasonic irradiation, as determined by sputtered neutral mass spectrometry. These data are a composite of many particles in the pellet at varying depths into each particle and therefore quantitatively underestimate the decrease in the oxide coating after ultrasonic irradiation. SNMS was chosen for these analyses because the propensity of Zn metal to volatilize in an electron beam precludes the use of other surface characterization techniques capable of better spatial resolution.

cleaning bath (<10 W/cm^2). When the complete reaction mixture is irradiated,[19] yields are >95% after 5 min at 25 °C. In contrast to previous work, iodine promotion had no effect in yield or reaction time.

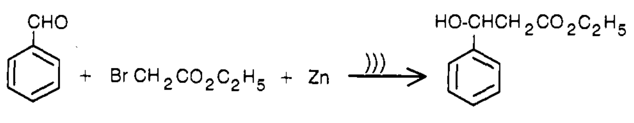

The effects of ultrasound are equally significant if the Zn powder is irradiated *before* the addition of substrate (Figure 1). The observed maximum rates (which occur at roughly 50% of completion) increase approximately 50-fold after ultrasonic irradiation for 15.0 min.[19b] In addition, the induction period observed is greatly reduced: in the absence of ultrasound, 1% product is formed only after more than 30 min; after 15 min irradiation, 1% product requires only 6 min.[19c]

This increase in activity is not due to increased surface area. Three-point B.E.T. determinations on irradiated Zn powders show only small increases in surface area (for 0-, 5-, 15-, and 30-min irradiation, 0.40, 0.46, 0.48, and 0.60 m^2/g ±5%), which cannot account for the large increase in reaction rates.

Scanning electron micrographs were taken of irradiated Zn samples (Figure 2). Dramatic changes in particle morphology and aggregation are observed. The Zn particles initially are extremely smooth and spherical, but upon sonication the surface is noticeably roughened. At the same time, particle agglomeration occurs, forming ≈50 μm aggregates within 30 min of irradiation.

Associated with these changes in surface morphology are changes in surface composition. Elemental depth profiles using sputtered neutral mass spectrometry[20] (SNMS) were obtained on Zn powders before and after ultrasonic irradiation (Figure 3). The appreciable oxide coating initially present on the Zn powder is significantly reduced after irradiation.

We believe that the observed changes in particle morphology, aggregation, and surface composition are due to high-velocity interparticle collisions. Ultrasonic irradiation of liquid-solid slurries creates shockwaves and turbulent flow which produces such collisions. If particles collide head-on, they can do so with enough energy to cause localized melting at the point of contact. This results in particle agglomeration and in the exposure of highly reactive Zn metal. If particles collide at a glancing angle, increased surface roughness and cracking of the oxide layer can result.[1a,9] The sonochemical activation of Zn powder comes from the loss of oxide passivation.

Acknowledgment. We appreciate the assistance of Dr. Irena Dulmer and Dr. Christopher Loxton at the Center for Microanalysis of Materials, UIUC, supported by the DOE under contract DE-AC-02-76ER-01198. Support of the National Science Foundation is greatly appreciated. K.S.S. gratefully acknowledges an N.I.H. Research Career Development Award and a Sloan Foundation Research Fellowship.

(19) (a) Each reaction solution was diluted with benzene, shaken with ice water, and neutralized with excess concentrated $NH_{3(aq)}$ until redissolution of the zinc salts occurred. The organic layer was isolated and diluted to a known volume; internal standard was then added, and the solution was analyzed by GC-MS on an HP 5970. (b) The interpolated maximum rates are 4.5, 24.5, 48.6, 97.2, and 220 mM/min after prior irradiation for 0.0, 1.0, 2.5, 5.0, and 15.0 min, respectively. (c) The interpolated induction times for formation of 1% product are 31.5, 16.0, 10.5, 8.5, and 6.0 min after prior irradiation for 0.0, 1.0, 2.5, 5.0 and 15.0 min, respectively. Interpolated induction times for the formation of 5% product are 41.0, 21.5, 13.0, 9.5, and 7.0 min, for the same conditions.

(20) (a) Oechsner, H. In *Thin Film and Depth Profiling Analysis*; Oechsner, H., Ed.; Springer: New York, 1983. (b) Reuter, W. In *SIMS V*; Benninghoven, A., Colton, R. J., Simons, S., Werner, H. W., Eds.; Springer: New York, 1986; pp 44, 94.

Metalloselective Anti-Porphyrin Monoclonal Antibodies

Alan W. Schwabacher,*[1] Michael I. Weinhouse, Maria-Teresa M. Auditor, and Richard A. Lerner

Department of Molecular Biology
Research Institute of Scripps Clinic
10666 North Torrey Pines Road
La Jolla, California 92037

Received October 12, 1988

Antibodies raised against transition-state analogues have recently been shown to catalyze acyl transfers and sigmatropic reactions.[2] This promising approach to enzyme-like catalysts can be extended in several ways. Different transition-state analogues will lead to antibodies catalyzing other reactions, and site-directed mutagenesis will undoubtedly allow improvement of catalytic efficiency and mechanistic understanding. Cofactors provide another approach.

Enzymes use cofactors to catalyze a wider variety of reactions than would be possible with protein alone.[3] Among the most versatile and interesting of these cofactors are the metalloporphyrins.[4] Synthetic metalloporphyrins can hydroxylate alkanes, mimicking the function of cytochrome P-450,[5] for example, but without the enzymatic specificity. We want to use antibody binding specificity to add substrate, regio-, and enantioselectivity to reactions catalyzed by metalloporphyrins.

Possibly an antibody raised against a porphyrin-substrate complex would have a binding site complementary to both and after binding to porphyrin would allow attack on only the correctly

(1) Address correspondence to this author at Department of Chemistry, Iowa State University, Ames, Iowa 50011.

(2) Janda, K.; Schloeder, D.; Lerner, R.; Benkovic, S. *Science* **1988**, *241*, 1187. Hilvert, D.; Nared, K. *J. Am. Chem. Soc.* **1988**, *110*, 5593. Schultz, P. G. *Science* **1988**, *240*, 426 and references therein.

(3) Walsh, C. *Enzymatic Reaction Mechanisms*; W. H. Freeman and Company; 1979.

(4) Dixon, M.; Webb, E. C. *Enzymes*, 3rd Ed.; Academic Press: 1979; Chapter IX.

(5) Groves, J. T.; Nemo, T. E. *J. Am. Chem. Soc.* **1983**, *105*, 6243.

0002-7863/89/1511-2344$01.50/0

Table I. Binding of MTCPP (1, R = OH) to Monoclonal Antibodies 35F8, 13C4, and 13B4[a]

	35F8		13C4		13B4	
M	K_D,[b] M	$\Delta\Delta G$,[c] Kcal/mol	K_D, M	$\Delta\Delta G$, Kcal/mol	K_D, M	$\Delta\Delta G$, Kcal/mol
H_2	2.6×10^{-5}	2.2	3.3×10^{-6}	2.7	5.9×10^{-5}	3.7
Mn^{3+}	1.3×10^{-5}	1.8	1.7×10^{-6}	2.3	4.7×10^{-6}	2.2
Fe^{3+}	3.2×10^{-5}	2.4	4.1×10^{-8}	0	1.4×10^{-7}	0
Co^{3+}	6.9×10^{-7}	0	1.4×10^{-5}	3.6	5.9×10^{-7}	0.9
Cu^{2+}	3.6×10^{-5}	2.4	1.5×10^{-5}	3.6	3.1×10^{-5}	3.3
Zn^{2+}	4.0×10^{-5}	2.5	1.3×10^{-4}	4.9	1.4×10^{-6}	1.4
Sn^{4+}	1.1×10^{-5}	1.7	3.0×10^{-5}	4.1	7.9×10^{-7}	1.1

[a] Binding determined at 37 °C in 10 mM pH 7.2 phosphate containing 150 mM NaCl and 15 mM BSA. [b] Binding determined by measuring inhibition of antibody binding to surface-bound protein-conjugated antigen by added MTCPP.[15] [c] Binding energy compared to the binding of antigen. Error limits are ±0.4 Kcal/mol.

oriented substrate. We envisioned the differences between states (with respect to oxidation state, nature and geometry of axial ligands, etc.) of a metal porphyrin involved in catalysis to be analogous to the differences between metal porphyrins containing different metals. If antibodies can distinguish between various metals in the porphyrin, we therefore expect the antibodies to affect the reactivity of bound porphyrin. Antibodies to flavins have been reported[6a] and have been recently shown[6b] to bind oxidized flavin more tightly than reduced flavin, thus shifting the redox potential. As anti-porphyrin antibodies were unknown, we needed to know whether they could be prepared, and, if so, whether there are metal-specific interactions.

We report here the preparation of metalloselective monoclonal antibodies to Fe^{3+} and Co^{3+} complexes of synthetic *meso*-tetrakis(4-carboxyphenyl)porphine (**1**), M = H_2, R = OH (TCPP), and the four order of magnitude range of the binding affinities of these antibodies to MTCPP (**1**) containing other metals.

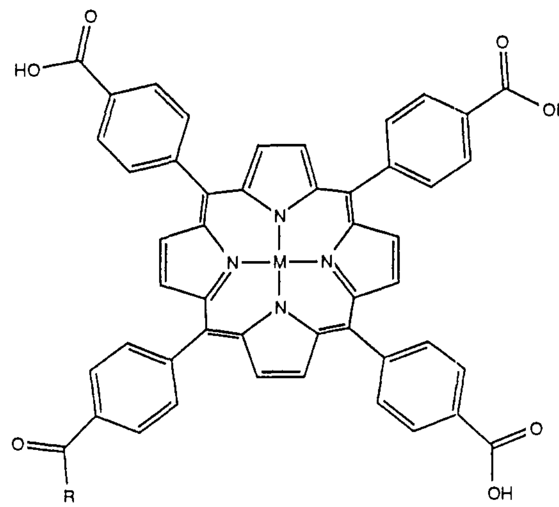

1

TCPP[7] was metalated with Fe^{3+} or Co^{3+} by standard methods.[8,9] Metalated porphyrins were activated, mainly at a single carboxyl, in DMF with 0.5 equiv of carbonyldiimidazole and coupled to the immunogenic carrier protein keyhole limpet hemocyanin (KLH) at pH 9 to yield **2**, M = Fe^{3+} or Co^{3+}, R = KLH. The conjugates were separated from excess porphyrin on sephadex G-50. Approximately 10–20 porphyrins were attached per KLH subunit.[10]

Bovine serum albumin (BSA) conjugates were similarly prepared and used to detect antibodies specific for the porphyrin.

Mice (Co^{3+} antigen Balb/C; Fe^{3+} 126 GIX$^+$ strain) were immunized with the KLH conjugates in complete Freund's adjuvant. Serum titer was determined with the BSA conjugate (**1**, R = BSA) by an enzyme-linked immunosorbent assay (ELISA).[11] Mice with a serum titer (the dilution at which half of the available ligand is bound to antibody) of 1:1600 were used to generate hybridomas by fusion of spleen cells with SP 2/0$^+$ myeloma cells by standard protocols.[12] Propagation of three of the resulting cell lines (35F8 (against Co^{3+}TCPP), 13C4 and 13B4 (against Fe^{3+}TCPP)) in mouse ascites (Balb/C or Balb/C × 129 GIX$^+$), ammonium sulfate precipitation, and DEAE Sephacel ion exchange chromatography at pH 8 gave monoclonal antibodies judged to be 90% pure by SDS-PAGE.[13]

Affinities of these monoclonal antibodies for their respective haptens, and other metalated TCPP,[7,8] were measured by a competitive[14] ELISA procedure[15] which has been shown to provide binding constants in agreement with other methods.

As can be seen in Table I, all three antibodies bind their eliciting antigens more strongly than they bind the porphyrin containing other metals. 35F8, raised against a Co^{3+} porphyrin, binds all other metals at least an order of magnitude less tightly but with only a 4-fold variation among the others. 13B4 binds other metals two to four orders of magnitude less tightly than Fe^{3+}TCPP.[16] 13C4 binds Fe^{3+}TCPP one to two orders of magnitude more tightly than the other metalated porphyrins.

The different patterns of specificity observed are of interest. In the anti-cobalt case (35F8), the metal plays a small role in determining binding specificity, and the unmetalated porphyrin is bound as well as the other metals, except for cobalt. In the case of 13B4, an anti-Fe^{3+} porphyrin antibody, although there is no obvious correlation of affinity with size or charge, there is a range of affinities, and the unmetalated porphyrin binds least well. This implies an interaction between the metal and the protein, though we cannot by this method distinguish between effects based on direct ligation of the metal, second-sphere interactions with axial ligands, and effects mediated through the porphyrin, such as

(6) (a) Farhangi, M.; Osserman, E. F. *N. Engl. J. Med.* **1976**, *294*, 177. (b) Shokat, K. M.; Leumann, C. J.; Sugasawara, R.; Schultz, P. G. *Angew. Chem., Int. Ed. Engl.* **1988**, *27*, 1174.

(7) Porphyrin products.

(8) Buchler, J. W. *Synthesis and Properties of Metalloporphyrins*. In *The Porphyrins*; Dolphin, D., Ed.; Academic Press: New York, 1978; Vol. I, Chapter 10.

(9) Cu^{2+}, Zn^{2+}: Pasternack, R. F., et al. *Inorg. Chem.* **1973**, *12*, 2606. Co^{3+}: Pasternack, R. F.; Parr, G. R. *Inorg. Chem.* **1976**, *15*, 3087. Fe^{3+}: Stong, J. D.; Hartzell, C. R. *Bioinorg. Chem.* **1976**, *5*, 219. Mn^{3+}: Ishii, H.; Koh, H.; Satoh, K. *Anal. Chim. Acta* **1982**, *136*, 347. Sn^{4+}: Vanderkooi, J. M.; Maniara, G.; Green, T. J.; Wilson, D. F. *J. Biol. Chem.* **1987**, *262*, 5476.

(10) Porphyrin concentration was estimated at pH 9 by Soret band absorption ($\epsilon_{408} = 9.96 \times 10^4$ M^{-1} cm^{-1} for Fe^{3+} μ-oxo dimer; $\epsilon_{427} = 1.72 \times 10^5$ M^{-1} cm^{-1} for Co^{3+}), assuming no change on coupling to KLH. Protein concentration was estimated by the method of Smith, P. K., et al. *Anal. Biochem.* **1985**, *150*, 76.

(11) Clark, B., Engvall, E. *Enzyme-Linked Immunosorbent Assay (ELISA): Theoretical and Practical Aspects in Enzyme-Immunoassay*; Maggio, E. T., Ed.; CRC Press: 1980; Chapter 8.

(12) Goding, J. W. *Monoclonal Antibodies: Principles and Practice*, 2nd ed.; Academic Press: 1986. Campbell, A. M. *Monoclonal Antibody Technology*; Elsevier: 1984.

(13) Smith, B. J. In *Methods in Molecular Biology*; Walker, J. M.; Ed.; Humana: NJ, 1984; Vol 1, Proteins, Chapter 6.

(14) One reason for a competitive procedure is that weak nonspecific binding of porphyrins to serum albumin and other proteins has been observed: Parr, G. R.; Pasternack, R. F. *Bioinorg. Chem.* **1977**, *7*, 277. Measuring binding competitively avoids this ambiguity.

(15) Friguet, B., et al. *J. Immunol. Methods* **1985**, *77*, 305. This method was compared with equilibrium dialysis and fluorescence transfer with good agreement.

(16) For the purposes of this paper, complications due to μ-oxo dimer equilibrium in the Fe^{3+} series were ignored.

distortion of the porphyrin from planarity. The other anti-Fe^{3+} porphyrin antibody, 13C4, demonstrates a four order of magnitude range of affinities for TCPP containing different metals, but the unmetalated porphyrin is one of those more tightly bound. Moreover, the Zn^{2+} and Sn^{4+} porphyrins, bound most weakly to 13C4, are among the most tightly bound to 13B4. A four order of magnitude range of affinities has also been observed in the binding of monoclonal antibodies to EDTA complexes of various metals.[17] The same range of affinities in anti-porphyrin antibodies is perhaps more surprising because the EDTA ligand is much more capable of conformational variability.

In summary, we have shown that monoclonal antibodies that bind tightly to porphyrins can be elicited. There is a large range of affinities possible for various metals, evidence of some kind of interaction, between metal and protein in antibody–porphyrin complexes, which may perturb the reactivity of a metalloporphyrin. Of particular importance for predictive correlations is the observation that in each case the metalloporphyrin used as the antigen is bound more tightly than the other porphyrins tested. We have shown that these antibodies can bind tightly to other metalloporphyrins related to the antigen. This is important because a catalytic porphyrin–antibody complex could result from immunization with a porphyrin containing a noncatalytic metal, chosen to stably bind a substrate. The next important step will be to bind a substrate as well as a porphyrin in an antibody binding pocket. Given more than 600 $Å^2$ of surface contact seen in antibody–protein complexes,[18] this may be possible.

Acknowledgment. This work was supported in part by the American Cancer Society in the form of a Postdoctoral Fellowship to A.W.S. We thank Diane Schloeder for advice on tissue culture.

(17) Reardan, D. T., et al. *Nature* **1985**, *316*, 265.
(18) Amit, A. G.; Mariuzza, R. A.; Phillips, S. E. V.; Poljak, R. J. *Science* **1986**, *233*, 747. Colman, P. M., et al. *Nature* **1987**, *326*, 358. Sherriff, S., et al. *Proc. Natl. Acad. Sci. U.S.A.* **1987**, *84*, 8075.

Alkyne Hydrogenation by a Dihydrogen Complex: Synthesis and Structure of an Unusual Iridium/Butyne Complex

Gregory Marinelli,† Idris El-Idrissi Rachidi,‡
William E. Streib,† Odile Eisenstein,*,‡ and
Kenneth G. Caulton*,†

Department of Chemistry and Molecular Structure Center
Indiana University, Bloomington, Indiana 47405
Laboratoire de Chimie Théorique, Bâtiment 490
Centre de Paris-Sud, 91405 Orsay, France

Received November 7, 1988

The η^2-H_2 ligand in $IrH_4P_3^+$ (P = PMe_2Ph) serves, in an equilibrium process, as a "good leaving group" and provides the rare *unsaturated* hydride complex $IrH_2P_3^+$. We reported earlier[1] the utilization of this species in a cycle for hydrogenation of ethylene at 25 °C and 1 atm. We describe here the use of this reagent for selective hydrogenation of 2-butyne, which leads to isolation of a butyne complex of remarkable structure.

Treatment of $[IrH_4P_3]BF_4$ in CH_2Cl_2 with 5 equiv of 2-butyne yields, as the only metal-containing product, $Ir(MeC_2Me)P_3BF_4$,[2] together with a mixture of *cis*-2-butene and 1-butene. Neither

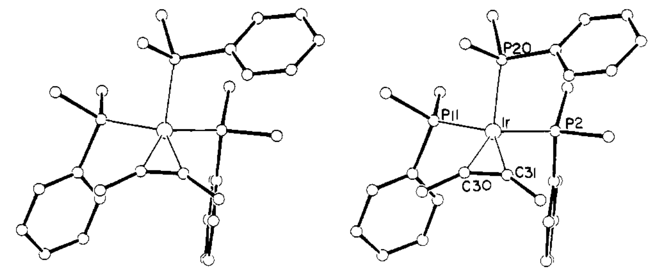

Figure 1. Stereo ORTEP drawing of $Ir(MeC_2Me)(PMe_2Ph)_3^+$, omitting hydrogen atoms. Selected structural parameters: Ir–P2, 2.309 (2); Ir–P11, 2.312 (2); Ir–P20, 2.236 (2); Ir–C30, 2.016 (5); Ir–C31, 2.014 (6); C30–C31, 1.306 (8) Å.

Scheme I

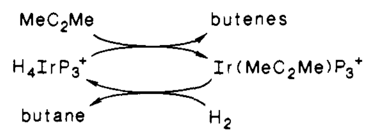

trans-2-butene nor butane is detected (^1H NMR). The ^1H NMR of this complex in CD_2Cl_2 shows only a single P-*Me* doublet at 22 °C, and the $^{31}P\{^1H\}$ NMR is a singlet from 22 °C to −95 °C. The apparent equivalence of the three phosphines,[3] which is reinforced by the quartet structure of both the Ir–C ^{13}C and the butyne proton signals, is surprising since we anticipated a structure based upon planar Ir(I) and a T-shaped IrP_3 fragment. We therefore determined the solid-state structure of $Ir(MeC_2Me)(PMe_2Ph)_3BF_4$ by X-ray diffraction,[4] which reveals noninteracting cations and BF_4 anions. The cation (Figure 1) has a structure which is neither planar nor tetrahedral: the IrP_3 fragment is distinctly nonplanar but also deviates markedly from C_3 symmetry.[5] The IrP(20) distance is 0.07 Å shorter than the two statistically equivalent IrP(2) and IrP(11) distances. Consistent with this approximate mirror symmetry are the PIrP angles, with those involving P(20) smaller (at 90.6 (1) and 94.0 (1)°) than those between P(2) and P(11) (106.1 (1)°). The line of the alkyne multiple bond is approximately parallel to the P(2)/P(11) vector. Thus, one description of the coordination geometry is square pyramidal (counting each alkyne carbon as one basal site of the polyhedron and P(20) as apical). The Ir–C distances are both very short (average value 2.015 (6) Å),[6] consistent with multiple bonds. The ^{13}C chemical shift of the alkyne carbons, 170.6 ppm, is in the range of four-electron donor alkynes.[7]

Bonding in the experimental (idealized C_s) structure was compared to idealized T_d and square-planar structures using extended Hückel theory calculations. This reveals the acetylene to be most tightly bound to the metal fragment (i.e., greater forward and back electron transfer) in the C_s structure. The differences originate in the superior match of the orbitals of the bent acetylene with IrP_3^+ in the C_s structure. The relevant donor orbitals of cis-bent acetylene ($\pi_\parallel$, in the IrC_2 plane and $\pi_\perp$, orthogonal to $\pi_\parallel$) are close in energy.[8] Of the two possible acetylene acceptor orbitals, only $\pi_\parallel^*$ is really effective. The "best prepared" d^8ML_3 fragment should therefore have two low-lying empty orbitals complementary to the symmetry of $\pi_\parallel$ and $\pi_\perp$ and a high-lying occupied orbital adapted to $\pi_\parallel^*$. The T-shaped IrP_3^+ fragment (leading to a square-planar structure) lacks the empty

† Indiana University.
‡ Centre de Paris-Sud.

(1) Lundquist, E. G.; Huffman, J. C.; Folting, K.; Caulton, K. G. *Angew. Chem., Int. Ed. Engl.* **1988**, *27*, 1165.

(2) NMR data (omitting phenyl resonances): ^1H NMR (360 MHz, 22 °C, CD_2Cl_2) δ = 2.85 (q, $^4J_{P-Me}$ = 3 Hz, 3 H); 1.66 (d, $^2J_{P-Me}$ = 10 Hz, 18 H); $^{13}C\{^1H\}$ NMR (125 MHz, CD_2Cl_2) δ = 170.6 (q, $^2J_{PC}$ = 5 Hz, *C*-Me), 19.9 (d, $^1J_{PMe}$ = 35 Hz), 18.5 (s, C-*C*H_3); ^{31}P NMR (146 MHz, 22 °C, CH_2Cl_2) δ = −16.8 (s). Yield of isolated product: 45%. Satisfactory elemental analysis was obtained for C, H, and P.

(3) A similarly simple spectrum is found in benzene-d_6 although the butyne methyl protons are shifted 0.4 ppm upfield from the value in CD_2Cl_2. The fact that this BF_4^- compound is soluble in benzene is, of course, surprising, and perhaps indicative of a structure with coordinated BF_4^-.

(4) Crystal data for $[Ir(MeC_2Me)(PMe_2Ph)_3]BF_4$ (−139 °C): a = 11.601 (1) Å; b = 13.855 (1) Å; c = 19.138 (3) Å; β = 99.66 (1)°; Z = 4 in space group $P2_1/n$. $R(F)$ = 0.0268 for 3610 reflections with $F > 3\sigma(F)$.

(5) A relevant comparison compound is $Co(PhC_2Ph)(PMe_3)_3^+$. See: Capelle, B.; Dartiguenave, M.; Dartiguenave, Y.; Beauchamp, A. *J. Am. Chem. Soc.* **1983**, *105*, 4662.

(6) Compare the Ir–C distance (2.159 Å) in *fac*-$IrMe_3(PMe_2Ph)_3$.

(7) Templeton, J. L.; Ward, B. C. *J. Am. Chem. Soc.* **1980**, *102*, 3288.
(8) Tatsumi, K.; Hoffmann, R.; Templeton, J. L. *Inorg. Chem.* **1982**, *21*, 466.

0002-7863/89/1511-2346$01.50/0